Fiducial Reference Measurements for Ground-Based DOAS Air-Quality Observations

ESA Contract No. 4000135355/21/I-DT-lr

Deliverable D8.3: BrO Validation Report

Date: 2026-07-31

Version: 1.0

Contributing authors:

Andreas Richter (IUP-UB)

Thomas Wagner (MPI)

Martina M. Friedrich (IASB-BIRA)

1 Table of Contents

2 Introduction

In this report, a first assessment of the FRM4DOAS BrO profile product is presented. This product, intended for the validation of satellite data from instruments such as Altius, is based on earlier work on deriving vertical BrO profiles from ground-based zenith-sky observations (Hendrick et al., 2008, 2009). However, the current processor is a new implementation and also uses different model data as a priori profiles.

Due to technical issues with the implementation and model output, only a limited dataset is available at this time. It consists of three years of data for Kiruna and two years for Harestua.

As there are no independent measurements of vertical BrO profiles available, this document cannot provide direct validation; instead, it focuses on internal consistency checks and comparisons with alternative retrievals, models, and satellite data. It is limited in scope and will be expanded on within the extension of the project.

3 Short description of data set

The data used for validation are netCDF files containing retrieval results for individual stations, separated by AM and PM. They include the retrieved profiles, the uncertainties, and the integrated vertical columns, separated for 80°, 85° and 90° SZA. Conversion between the three profiles is done with the a priori model, which in this case is the BASCOE model.

The files also contain the original slant columns and the modelled slant columns after the profile inversion. However, these data have not been used in this report.

In addition to profile uncertainties, flags are provided to enable user-defined data filtering. Three different flags are provided, which are partially overlapping:

- RMS flag. This flag will be raised if the relative rms of one of the three retrievals is larger than 1.3
- DOF flag. This flag will be raised if the number of degrees of freedom for one of the profile inversion is less than 1.5
- Consistency flag. This flag will be raised if the difference between the VCDs retrieved at the three SZAs is larger than the VCD error.

The flags are also all raised in case of missing retrievals.

4 Analysis of the internal consistency of the data sets

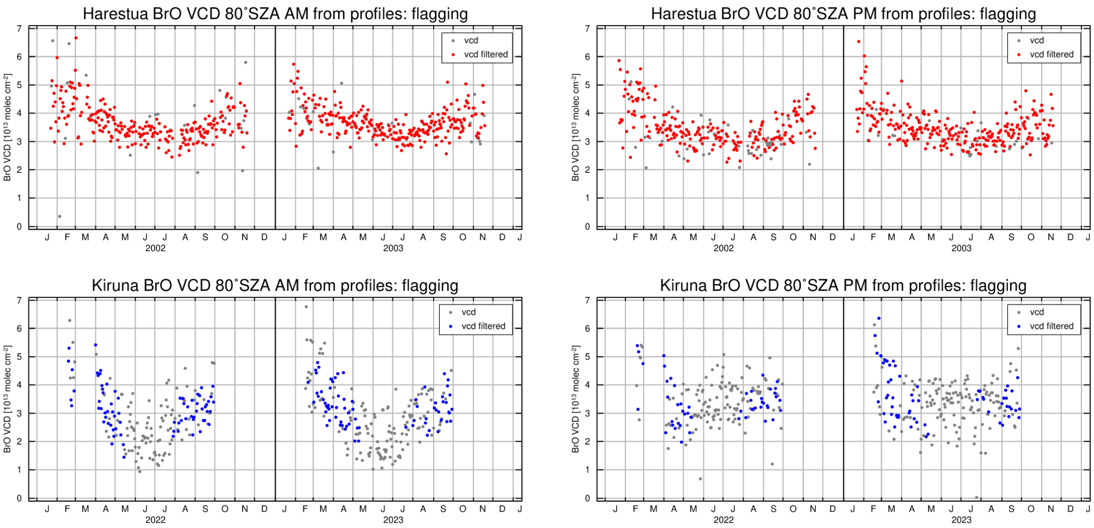

Figure 1: Overview of BrO VCDs at 80° SZA from the profiles for Harestua (top) and Kiruna (bottom).AM values are shown left, PM values right. Coloured points indicate retrievals that passed the flagging, grey points raised at least one error flag.

As a first test, the BrO vertical columns retrieved for the two stations are plotted in Figure 1, separated into AM and PM values. For Harestua, the values show the expected behaviour with larger values in winter and lower values in summer. The values of the BrO columns vary between about 2x10^{13} and 6x10^{13} molec cm^{-2} with a scatter in the order of 1x10^{13} molec cm^{-2}. The behaviour in both years is comparable, as are the values retrieved for the morning and for the evening, the latter being slightly lower. As mentioned above, the files contain flags for user defined filtering. In Figure 1, data points for which at least one of the flags is raised are shown in grey colour. As can be seen, very few data points are flagged as poor retrievals, and most of the obvious outliers are removed by the flags.

The data for Kiruna (also shown in Figure 1) are characterised by a larger variability. The seasonal variation is similar to that in Harestua, in that summer values are lower, but it is much stronger in the morning than in the afternoon. The two years shown behave similarly, both with respect to absolute values and day-to-day variability. One important difference from the results found for Harestua is the fact that nearly all summer values are flagged as bad. This is linked to the difference in SZA range covered – in summer, 90° SZA is not reached in Kiruna.

A more detailed overview of the effect of flagging is shown in Figure 2. In Harestua, only a small number of retrievals are flagged, and this includes some obvious outliers. There is no clear pattern in which values are flagged by which criteria, so combining them appears to be the best choice. In Kiruna, the most obvious effect is the flagging of all summer values, for which there are no 90° SZA observations. As in such cases all flags are raised, there is no additional information from the individual flags. Outside the summer months, more data are flagged than in Harestua. This is true for the rms flag, particularly in spring, but also the consistence flag, which flags many values in August. The results for PM retrievals (not shown) are similar.

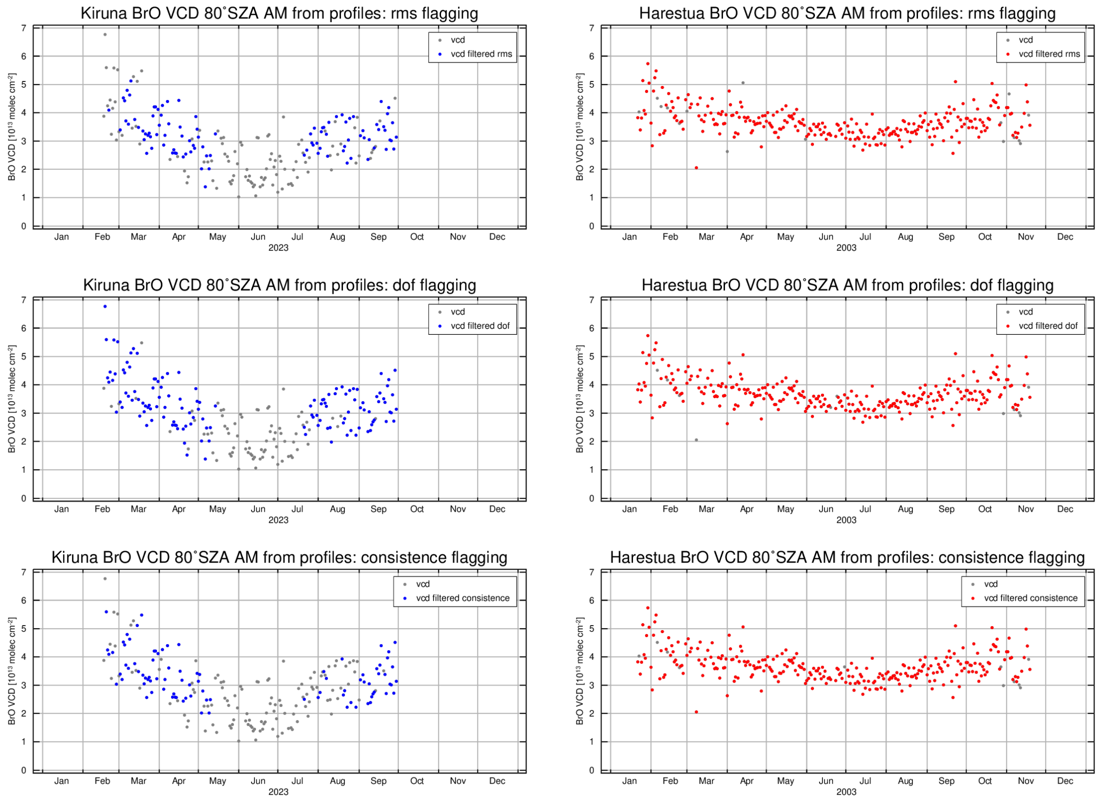

Figure 2: Effect of different flags on the number of valid data for one year of data in Kiruna (left) and Harestua (right). Retrievals are for 80° SZA AM. Coloured points are valid with respect to the flag evaluated; grey points are invalid.

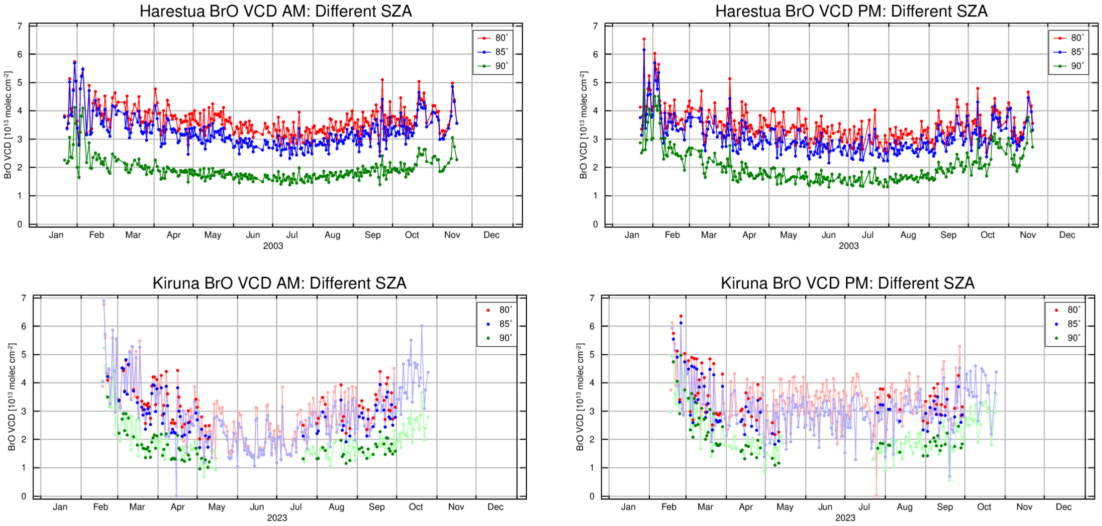

Figure 3: Evolution of the BrO vertical columns with retrieval SZA. Top: Harestua, bottom: Kiruna. AM values are shown left, PM values right. For Harestua, only unflagged values are shown; for Kiruna, also flagged values are shown in light colours.

A second consistency test is the comparison of the BrO columns retrieved at different solar zenith angles. As shown in Figure 3 for one year, the retrieved vertical columns decrease as the solar zenith angle increases. This is due to the rapid BrO photochemistry in the stratosphere. It is also interesting to note that while the relative changes remain similar, the absolute day-to-day variations get smaller as the SZA increases. This could imply that BrO vertical columns are less sensitive to dynamical changes and more determined by photochemistry at twilight. While the absolute values decrease with SZA, the seasonality appears to increase, particularly for PM values, as the SZA dependence of the BrO columns is weaker in winter than in summer. All of the above is valid for both Harestua and Kiruna.

The summary of this first quick look is that the data product appears consistent at first glance, that data in Harestua show less variability and that the flagging works as expected in Harestua but removes many retrievals in Kiruna.

5 Comparison of the BrO dSCDs from different fit windows

The study by Aliwell et al. (2002) recommended using a fit range including 2 BrO absorption bands. At that time, extending the fit range towards shorter wavelengths was not readily possible due to strong ozone absorption, especially at high SZA. In the last decade, however, DOAS spectroscopy was improved, in particular by including higher-order correction terms as suggested by Pukite et al. (2010) and Pukite and Wagner (2016). Thus, also BrO retrievals including 3 or 4 BrO absorption bands became possible (see Figure 4). In the following, we compare the results of three analyses including 2, 3, or 4 BrO absorption bands. The corresponding fit settings are provided in Table 1. We apply the BrO DOAS analyses to zenith sky observations in Kiruna (northern Sweden). During the considered period from 1995 to present the spectrometer stayed unchanged, but in 2013 the original photodiode detector was replaced by a CCD detector (for more details see Wagner et al., 2026). Exemplary fit results for measurements with both detectors are shown in Figure 5.

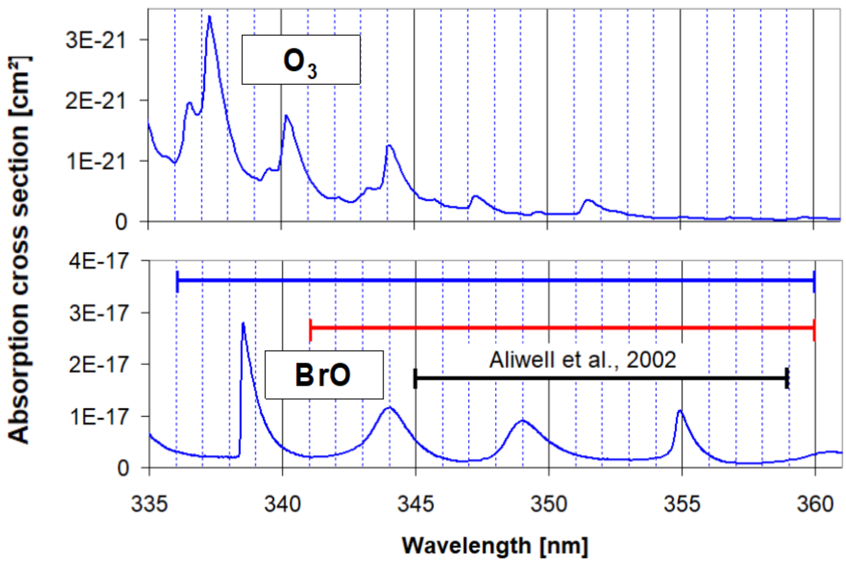

Figure 4: Absorption cross sections of BrO and O_3 in the UV spectral range. Also indicated are the spectral ranges for BrO analyses including 2, 3, or 4 bands.

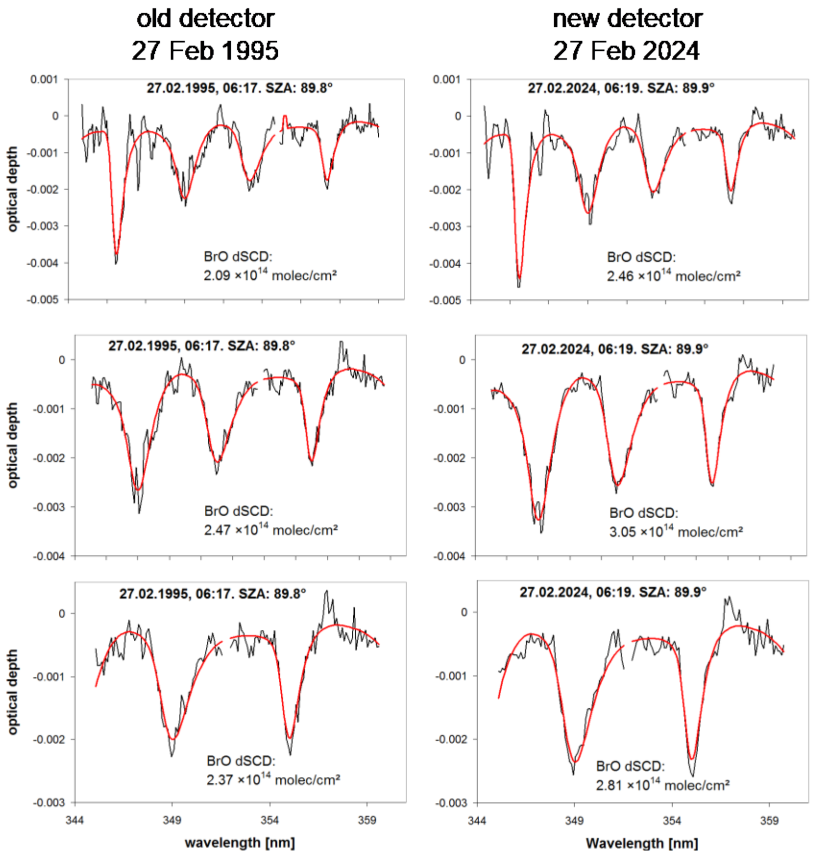

Figure 5: BrO fit results for measurements with the old (left) and new (right) detector for the different fit ranges.

Table 1: Reference spectra and further fit parameters used for the BrO analyses covering 2 to 4 BrO bands in the fitting ranges 345 – 360 nm, 341 – 360 nm, and 336 – 360 nm, respectively. The settings from Aliwell et al. (2002) are also shown.

Reference spectrum / parameter	2 bands	3 bands	4 bands	Aliwell et al., 2002 346 – 359 nm
BrO 228 K (Wilmouth et al. 1999), convolution	√	√	√	BrO 228 K Wilmouth et al. 1999
OClO 213 K (Kromminga et al. 2003), convolution	√	√	√	Should be included for high latitude
NO_2 220 K (Vandaele et al. 1998), I_o correction (10^{17}molec/cm²)	√	√	√	NO_2 227 K Harder et al. 1997
O_4 273 K (Thalman and Volkamer, 2013), convolution	√	√	√	O_4 298 K Greenblatt et al., 1990
O_3 223 K* (Bogumil et al. 2003), I_o correction (10^{20} molec/cm²) after ‚de-convolution’	√	√	√	O_3 221 K Burrows et al., 1999
O_3 243 K* (Bogumil et al. 2003), I_o correction (10^{20} molec/cm²) after ‚de-convolution’	√	√	√	O_3 241 K Burrows et al., 1999
Ring spectrum calculated from measured spectra (Wagner et al., 2009a)	√	√	√	Chance and Spurr, 1997
Ring spectrum multiplied by λ^4	-	√	√	-
Ring spectrum for O_3 calculated for O_3 cross section of 223 K	-	-	√	-
O_3 Pukite square term for O_3 cross section of 223 K (Pukite et al. 2016)	-	√	√	-
O_3 Pukite wavelength term for O_3 cross section of 223 K (Pukite et al. 2016)	-	√	√	-
DOAS polynomial	3th order	5th order	5th order	2nd order
Intensity offset and dependencies on wavelength	Constant and linear terms	constant, linear, and square terms	constant, linear, and square terms	Constant and linear terms

*the original O_3 cross sections were deconvolved before the I_o correction (as in Vandaele et al., 2005)

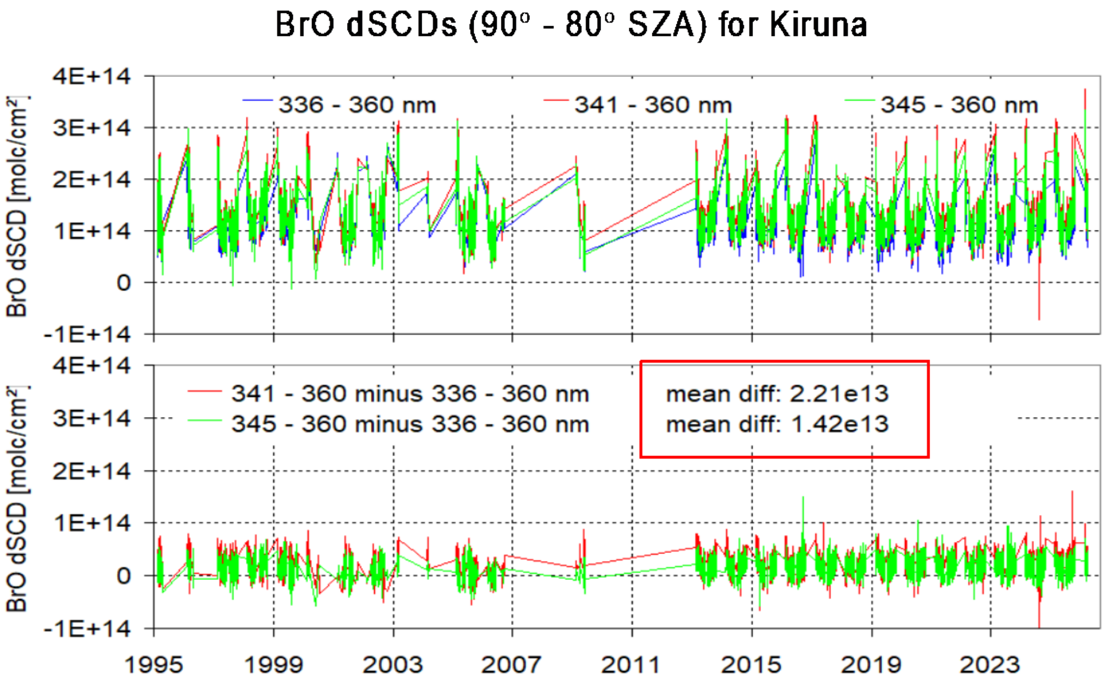

Figure 6: Top: BrO dSCDs (90° versus 80° SZA) for the different fit ranges; bottom: differences with respect to the results for the largest fit range (336 - 360 nm).

In Figure 6, time series of BrO dSCDs for 90±0.5° SZA analysed with daily Fraunhofer reference spectra at 80° SZA are presented. The results for the different fit ranges show very similar temporal variability, but differ systematically in their absolute values. The differences stay almost constant with time.

In addition to the retrieved BrO dSCDs, further fit results were compared to assess the quality of the DOAS analyses across different fit ranges (Figure 7). The highest RMS is found for the largest fit range, likely due to increased O_3 absorption and lower light intensity at shorter wavelengths. The RMS for measurements with the new detector is much smaller than for the old detector because of the higher quantum efficiency of the new CCD detector (see above). Interestingly, the fit error shows the opposite behaviour: the smallest fit error is found in the analyses with the largest fit range. This finding indicates that the larger spectral range has a higher spectral information content, which overcompensates for the increased RMS. For the fitted intensity offset, the smallest (absolute) values are found for the analysis with 2 BrO bands (345 - 360 nm).

Based on these results (and also those of section 6), either the small fit range (345 - 360 nm) with 2 BrO bands or the large range (336 - 360 nm) with 4 BrO bands is recommended.

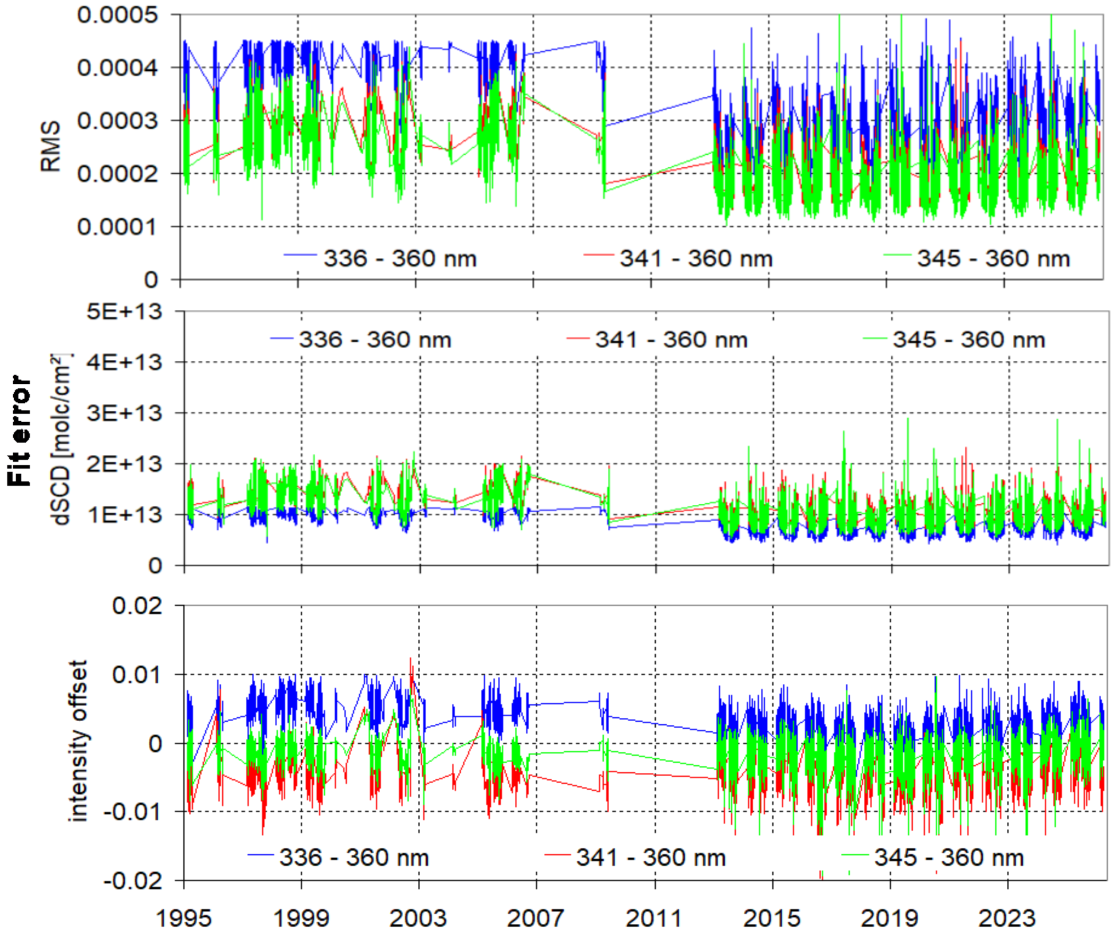

Figure 7: RMS (top), fit error (middle), and intensity offset (bottom) for the different fit ranges. Before 2011, measurements were carried out using a photodiode array detector with lower quantum efficiency than the new CCD detector after 2013.

6 Dependence of the BrO results on the tropopause height

It is a well-known phenomenon that the O_3 column changes systematically with variations in tropopause height (e.g., Theys et al., 2009; Sihler et al., 2012). In a simplified view, this variation can be explained as follows: if the tropopause height increases, the stratospheric O_3 profile shifts upward, while its mixing ratio remains nearly unchanged. Because of the decrease in air density with height, the O_3 concentration also decreases, leading eventually to a decrease in the O_3 total VCD. This relationship is also confirmed for Harestua and Kiruna, see Figure 8. Here the tropopause heights are derived on a daily basis from measurements of the AIRS satellite instrument (AIRS Science Team, 2013) and obtained via the GIOVANNI database (https://giovanni.gsfc.nasa.gov/giovanni/). The ozone data were derived from the MERRA model (GMAO, 2015) and also obtained via the GIOVANNI database. For Kiruna, O_3 VCDs derived from zenith sky observations using the Langley-plot method are also included. In Figure 9, the corresponding correlation plots are shown. Before the correlations are calculated, the ozone data are first normalised (divided) by the average seasonal cycle (described by a fitted 2nd order polynomial). A similar normalisation was applied to all further trace gas datasets before calculating the correlations with tropopause height (the normalised quantities are referred to as 'VCD ratios', see below).

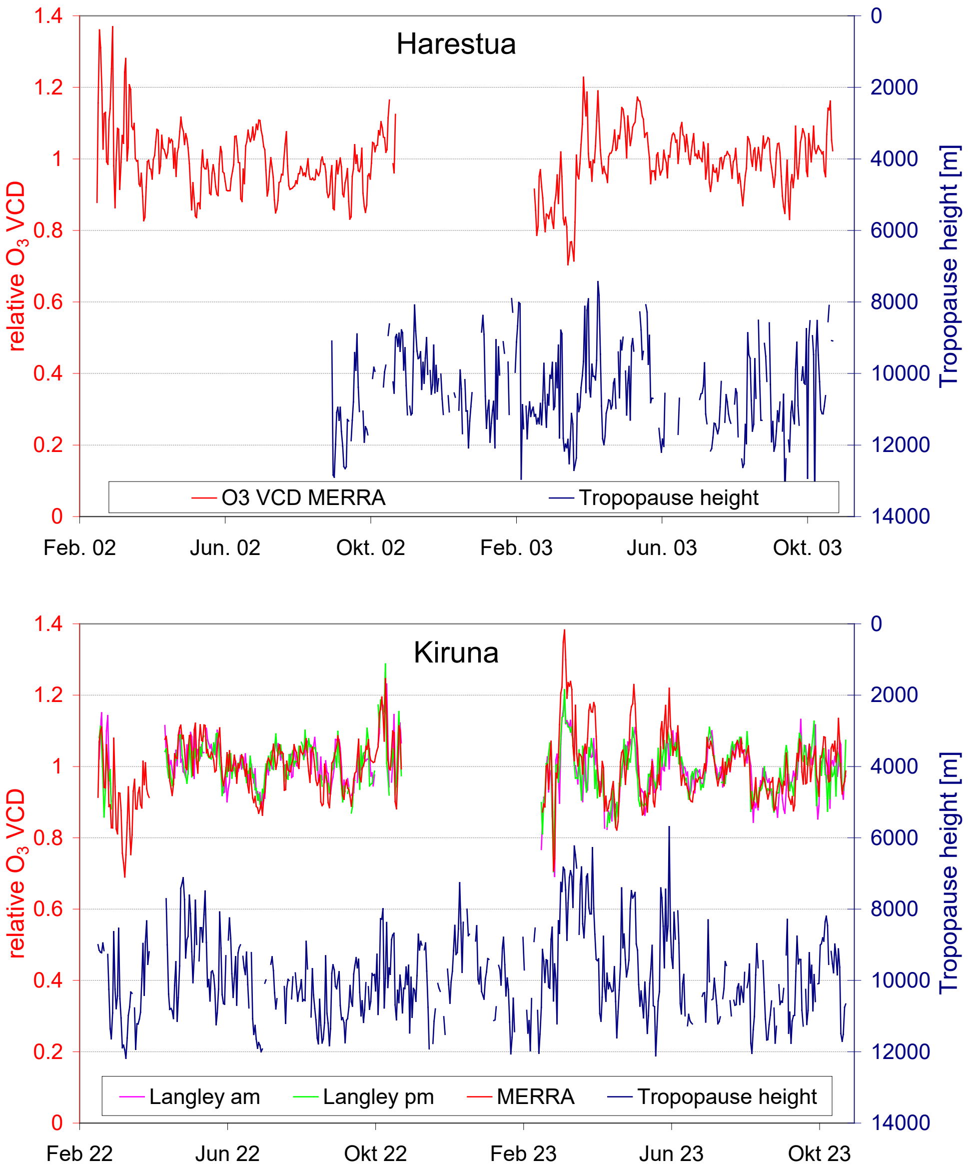

Figure 8: Comparison of the O_3 VCDs (left y axes) and tropopause heights (right axes, inverted) for Harestua (top: 2002 & 2003) and Kiruna (bottom, 2022 and 2023).

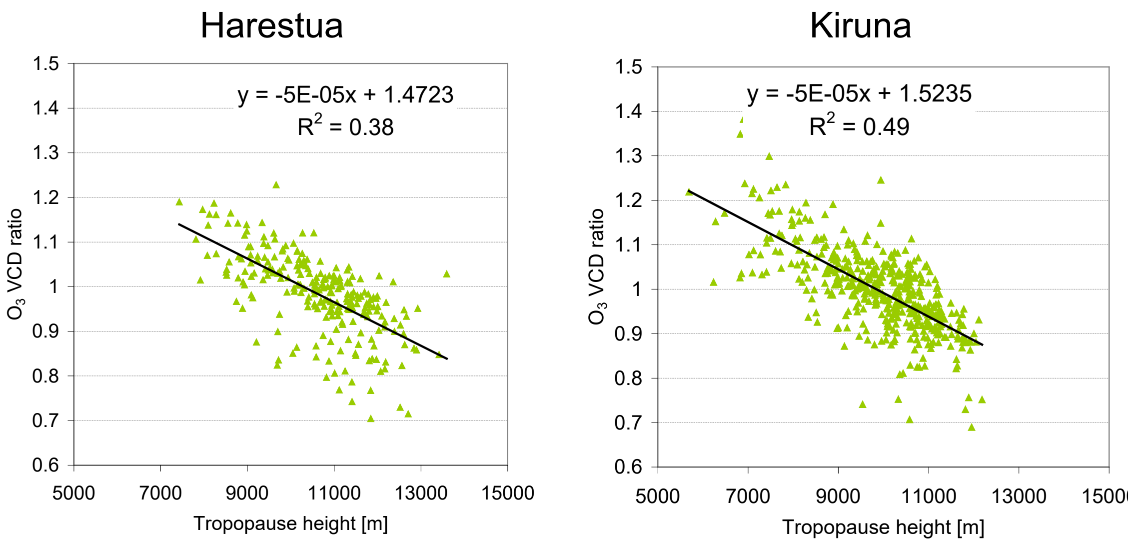

Figure 9: Correlation plots of the data shown in Figure 8. The ozone data were normalised to remove the seasonal cycle (see text).

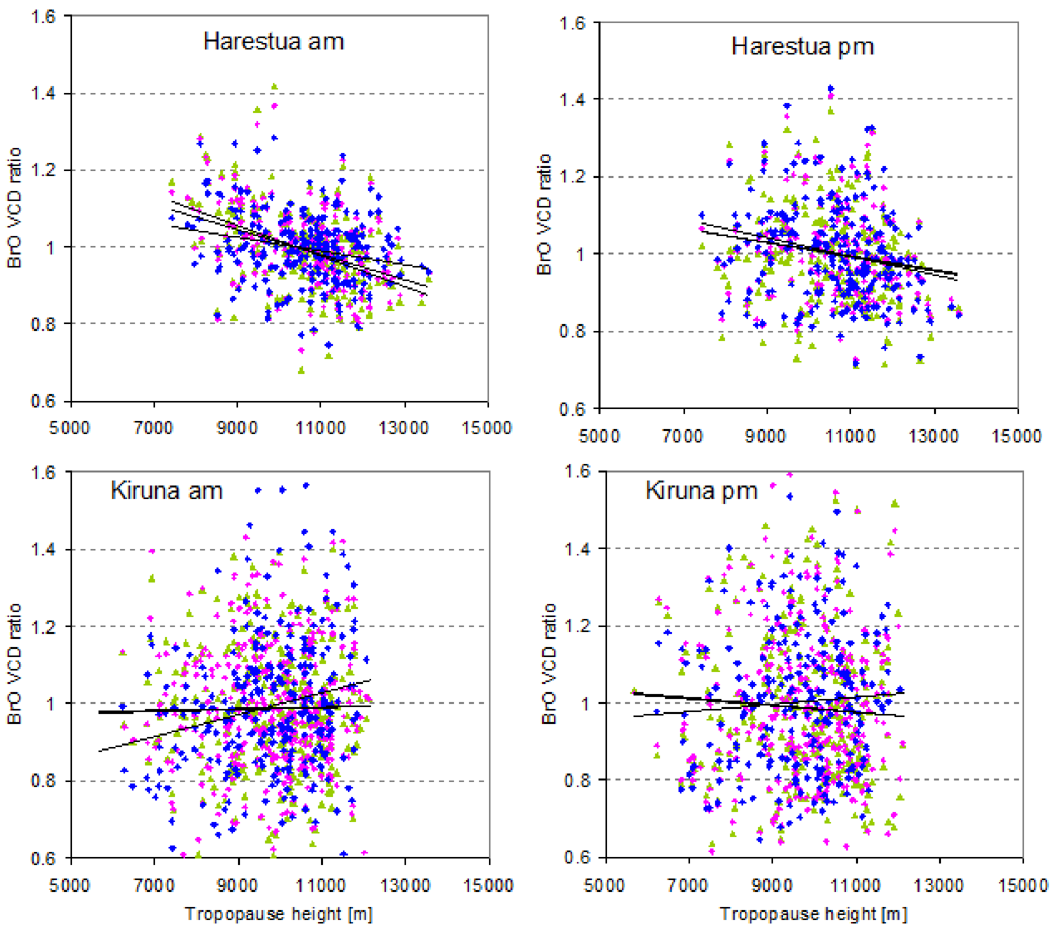

Figure 10: Correlation plots of the normalised BrO VCDs derived from the profile retrieval algorithm versus the tropopause height for the measurements at Harestua (top) and Kiruna (bottom). Green, magenta, and blue markers represent results for 80°, 85°, and 90° SZA, respectively.

Since similar arguments also hold for the stratospheric BrO profile (which is located even closer to the tropopause), this section investigates the dependence of the retrieved BrO VCDs at Harestua and Kiruna as an independent verification of the BrO profiling algorithm. Note that no flags were applied, but a few (<10) obvious outliers were removed manually. The corresponding results are shown in Figure 10. Interestingly, only a weak correlation (r^2 between 0.03 and 0.17 for Harestua) or almost no correlation (r^2 between 0 and 0.04 for Kiruna) is found. The results in Figure 11 are obtained for the BrO fit range 345–360 nm, but similar results are also found (for Kiruna) for fit ranges that include 3 or 4 BrO bands.

The weak correlations found for the BrO VCDs from the profile retrievals were also surprising, since for the BrO VCDs retrieved from satellite or from ground (using a fixed Fraunhofer reference spectrum), much higher correlations were obtained (Figure 11). Here, for the ground-based measurements, spectra at 80±0.5° SZA were analysed. The satellite data are from the TROPOMI BrO retrievals (Seo et al., 2019) and computed from the slant columns assuming a purely stratospheric BrO profile. In Figure 12 it is shown that for SZA around 80° the correlation is highest. The decrease of the correlation towards smaller SZA is probably caused by the weaker BrO absorption for the shorter atmospheric light paths. The decrease of the correlation towards higher SZA is probably caused by the lower sensitivity of the measurements towards the lower parts of the BrO profile (see Figure 13).

Finally, the consistency of the daily am and pm BrO VCDs derived from the different methods is investigated (Figure 14). Again, for the BrO VCDs from the profile inversion, only weak (Harestua) or no (Kiruna) correlation was found. Interestingly, for the Kiruna results obtained from the analysis with fixed Fraunhofer reference spectrum or from the Langley-plot method, much higher correlations were obtained.

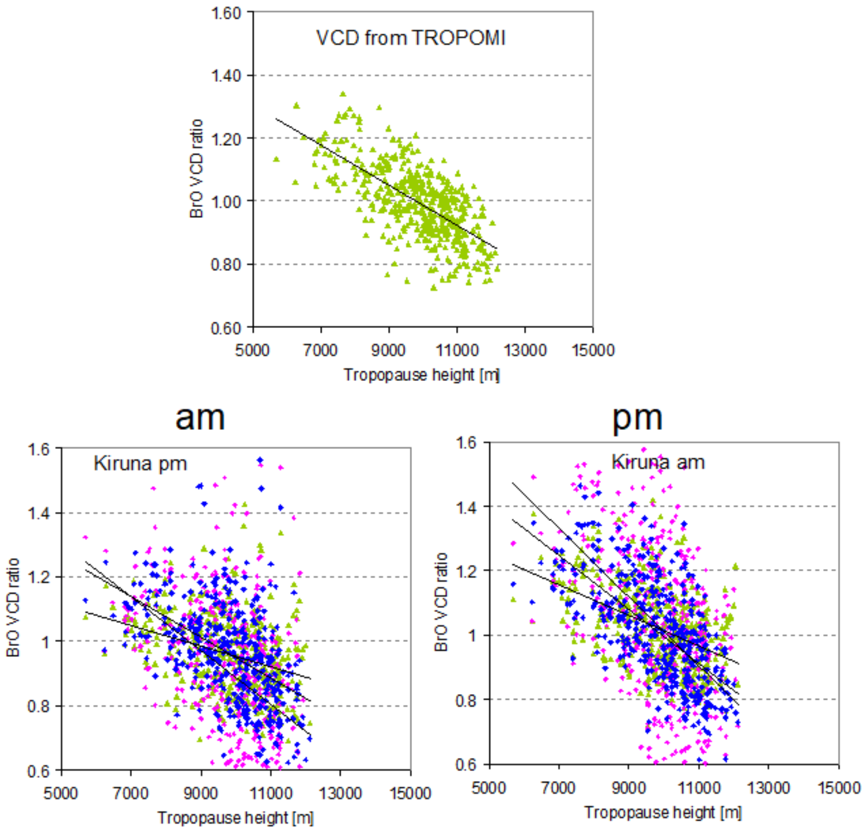

Figure 11: Correlation analyses of the normalised BrO VCDs retrieved from satellite (top) or from ground (bottom, using daily measurements at 80±0.5° SZA and a fixed Fraunhofer reference spectrum from 23rd February at 80° SZA). Green, magenta, and blue markers represent results for the fit ranges with 4, 3, or 2 BrO bands, respectively. The correlation coefficients (r^2) are 0.45 for the satellite data, and between 0.10 and 0.39 for the ground-based data. The highest and lowest correlations are found for the fit ranges 345-360 nm and 341-360 nm, respectively.

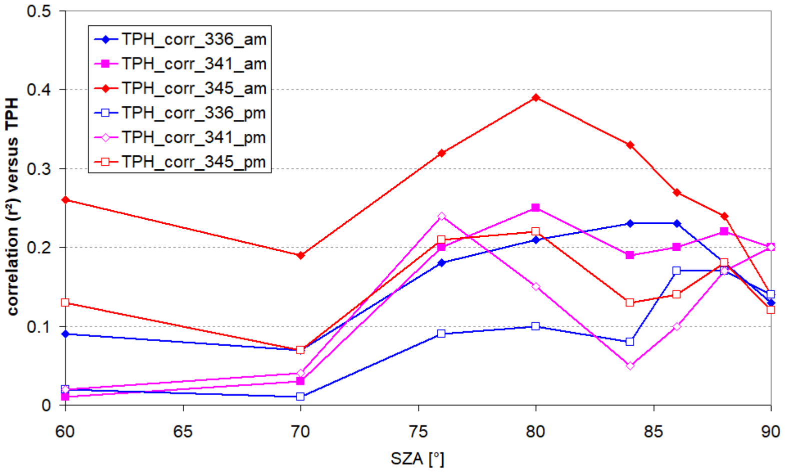

Figure 12: Obtained correlation coefficients (r^2) versus tropopause height for BrO results from the ground-based measurements analysed with a fixed Fraunhofer reference spectrum for am and pm measurements at different SZA.

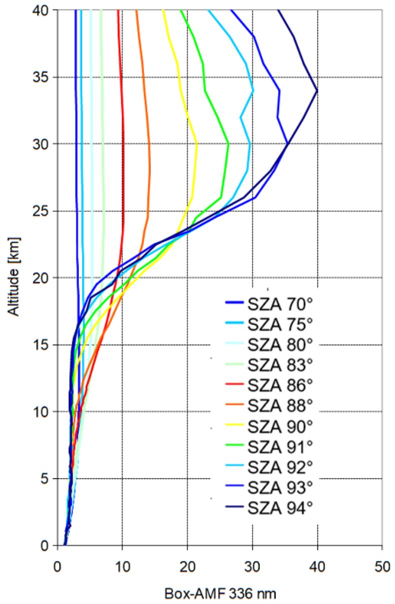

Figure 13: Box-AMF (336 nm) for zenith-sky measurements of BrO for different SZA. The sensitivity for the lower part of the BrO profile decreases with increasing SZA.

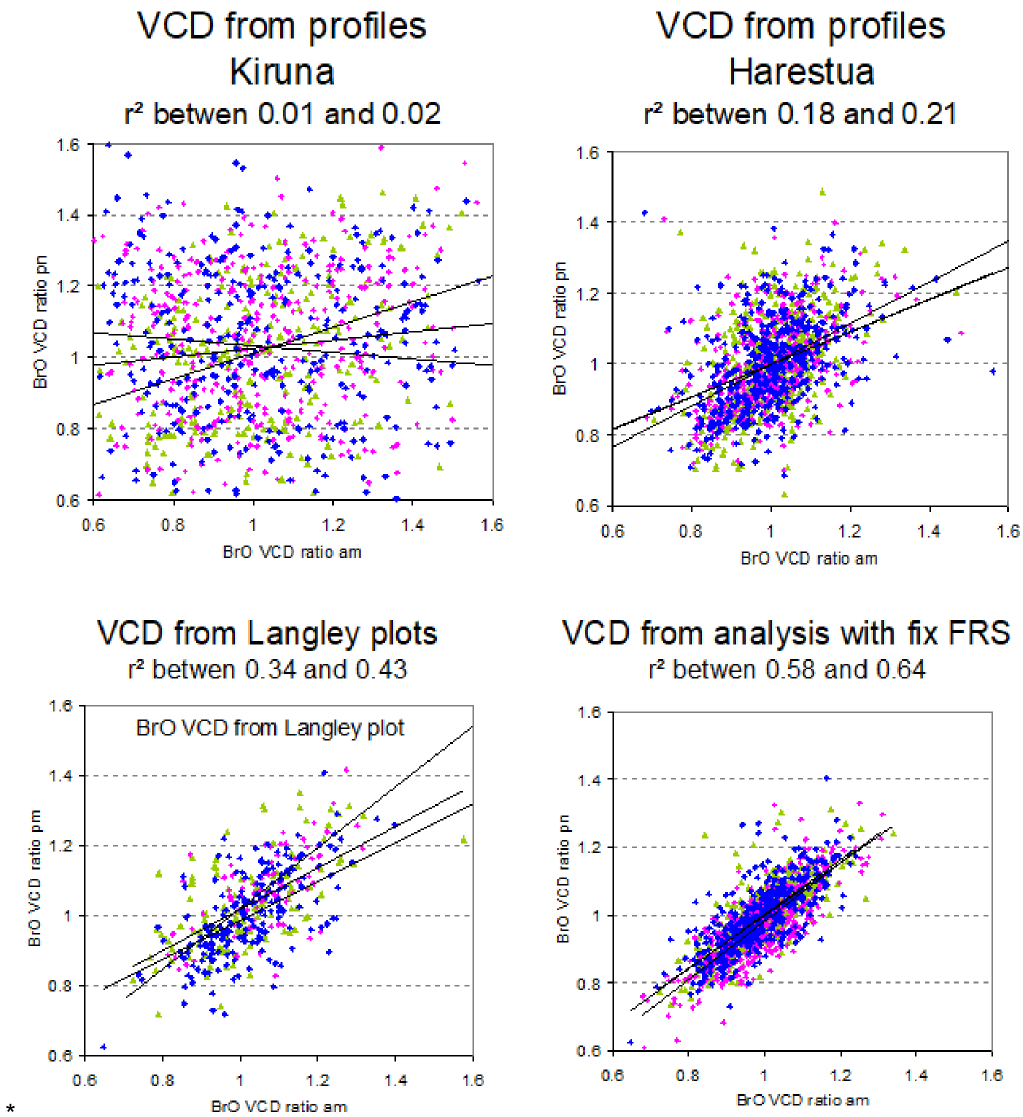

Figure 14: Correlation of the pm versus am BrO VCDs for different locations and methods. Top: BrO VCDs derived from the profile inversion for Harestua and Kiruna. Green, magenta and blue markers represent results for 90, 85, and 80° SZA, respectively. Bottom: BrO VCDs from the Langley-plot method (SZA: 70 – 89°) and analysis with a fixed Fraunhofer reference spectrum. Green, magenta, and blue markers represent results for the fit ranges with 4, 3, or 2 BrO bands, respectively.

From the findings of this section, the following conclusions are derived: while for BrO VCDs obtained from satellite observations or ground-based observations with a fixed Fraunhofer reference spectrum a reasonable correlation with tropopause height was found, the correlations of the BrO VCDs retrieved from the profile retrievals were much lower (even close to zero for the Kiruna observations). Also, for the am/pm comparison, lower correlations were found for the BrO VCDs from the profile retrieval compared to the BrO VCDs from the analysis with fixed Fraunhofer reference spectrum (or using the Langley-plot method).

Both findings indicate that there might still be room for improvement for the BrO profiling algorithm.

The correlation results were particularly low for Kiruna. This finding is currently not well understood. But there are important differences for the profile retrievals at both locations. First, the Harestua data were analysed using daily Fraunhofer reference spectra for the lowest SZA of each day, while the Kiruna data were analysed against measurements at a fixed SZA of 80°. These differences will especially have a systematic influence on the currently applied normalised RMS filter, since its calculation includes the reported fit error, which is much smaller for the Kiruna measurements. It is therefore suggested to use the non-normalised RMS as a quality filter in the future. Also, as shown in section 3, the currently applied quality filters remove almost all data for Kiruna during summer. This is mainly caused by the absence of high (>90°) SZA during polar day. In the future it should be investigated whether under such conditions still meaningful BrO profiles (or at least BrO VCDs) could be retrieved, and how the quality filters might be relaxed accordingly. Probably, under such conditions, no meaningful BrO profiles can be retrieved for a reference SZA of 90°. Future studies should investigate which reference SZA could be chosen instead, and for which set of SZAs meaningful consistency criteria could be applied.

In addition, the results of the chemical transport model used in the profile inversion algorithm might have larger uncertainties for the high-latitude station of Kiruna because of the complex photochemistry during the long twilight periods in Summer. Also these aspects should be further investigated in future studies.

7 Comparison of retrieved BrO VCDs with satellite data

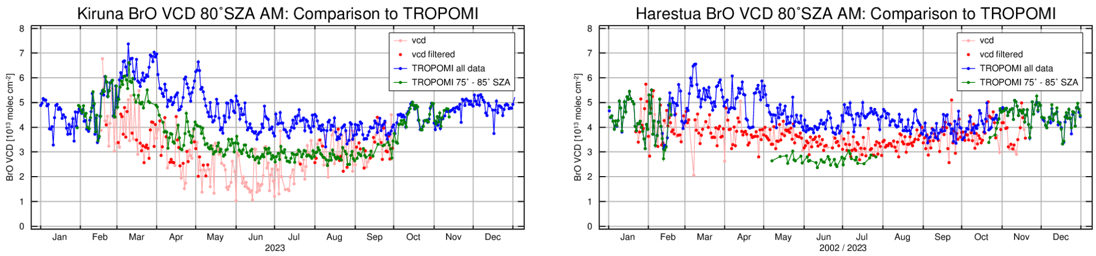

Figure 15: Comparison of BrO columns retrieved for Kiruna for 80° SZA and TROPOMI satellite columns in a 100 km radius around Kiruna. The blue line is the average over all measurements from the TROPOMI daylight scan, the green curve is the average over all measurements with solar zenith angles between 75° and 85°. Ground-based data are colour coded for their flagging status, with full red points indicating retrievals with no flag raised. Please note that for Harestua, the ground-based retrievals are for 2003 while the satellite data are for 2023.

It is interesting to compare the retrieved BrO columns with results from the TROPOMI satellite instrument. For the Kiruna data set, the available ground-based data overlap temporally with the TROPOMI time series. Some comparisons were already shown in Figure 11. Here, we focus on the seasonality and the absolute values.

As shown in Figure 16, for Kiruna, the satellite columns (blue line) are larger than the ground-based retrievals for AM 80° SZA (red line). It is, however, important to consider the measurement conditions and the averaging applied to the satellite data. To improve the signal-to-noise ratio, all TROPOMI measurements within a 100 km radius around Kiruna have been averaged. This smooths out spatial variability and, in winter, shifts the effective latitude southward, where the solar zenith angle is smaller. This explains why there is TROPOMI data in months with no ground-based retrievals. Over the course of the year, the solar zenith angle of the TROPOMI measurements changes and is systematically lower than 80°SZA, the angle for which the retrievals were performed.

An alternative TROPOMI data set is shown in green. These data are averaged only over measurements between 75° and 85° SZA, reducing the SZA difference between the two data sets. While this reduces the gap between ground-based and satellite data, particularly in August and September, it does not fully eliminate the discrepancy. The difference between ground-based and satellite data is reduced from more than $2x10^{13}$ molec cm^{-2} to about $1x10^{13}$ molec cm^{-2}. It should be noted that during summer, TROPOMI 80° SZA measurements are from the descending part of the orbit, which may have larger uncertainties due to a different viewing geometry (different relative azimuth and local time compared to other satellite data).

For Harestua, a direct comparison between ground-based retrievals and TROPOMI data is not possible due to the lack of temporal overlap. Therefore, the data shown for Harestua in Figure 16 are 20 years apart, and can only be compared in a qualitative way. As was the case for Kiruna, satellite columns are larger than ground-based retrievals most of the year. However, in January and February as well as September and October, the agreement is good. There are fewer TROPOMI measurements around 80° SZA available for Harestua because it is at a lower latitude. TROPOMI data at 80°SZA are lower than those at larger SZA, and in Harestua are even lower than the ground-based retrievals.

8 Comparison of retrieved BrO VCDs with 3D-CTM model data

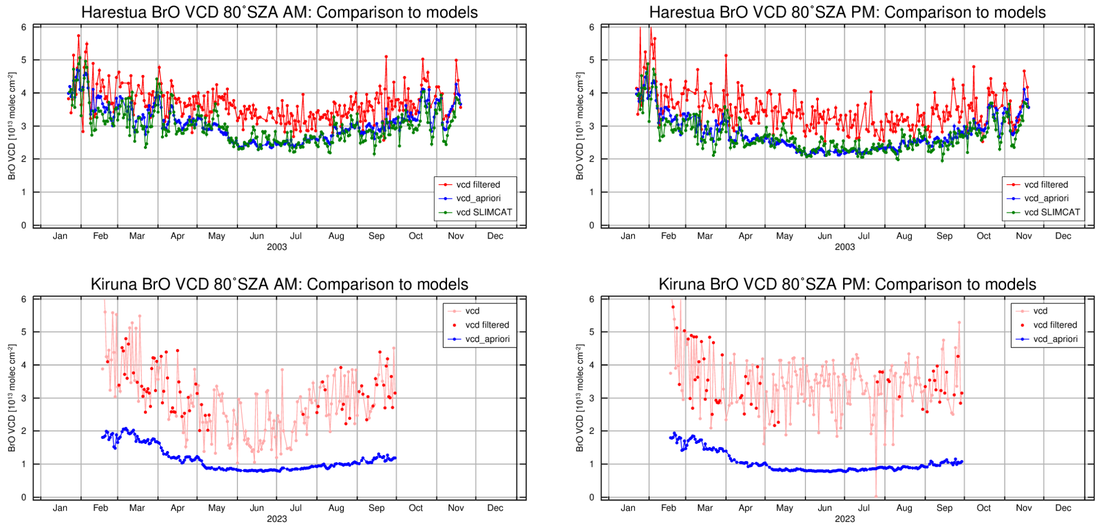

Figure 16: Comparison of the BrO VC from the profile retrieval (red) to model columns from BASCOE (blue) and SLIMCAT (green). Top: Harestua, bottom: Kiruna. AM values are shown left, PM values right. For Harestua, only unflagged values are shown; for Kiruna, flagged values are shown in light colours.

It is interesting to compare the retrieved BrO columns with model results. Two different models are available for this comparison: the BASCOE model, which is used as a priori and for the photochemical calculations in the retrieval, and for Harestua also SLIMCAT. As shown in Figure 16 for Harestua, the two models agree very well; the main differences are a larger short-term variability in the SLIMCAT data and slightly more pronounced seasonality in the BASCOE data. Comparison between retrievals and models shows very good agreement in the overall shape but an offset of about 1×10^{13} molec cm^{-2}. In addition, there is greater variability in the retrievals than in the model, either due to better spatiotemporal resolution of the measurements or as a result of observational noise.

For Kiruna, only the BASCOE data are available. While the retrieved BrO columns in Kiruna are of similar magnitude as those in Harestua, the BASCOE model predicts much lower columns. There is also a large difference in day-to-day variability, presumably due to a lower signal-to-noise ratio in the data from Kiruna. The seasonality of the two data sets is in qualitative agreement, but there is a large offset.

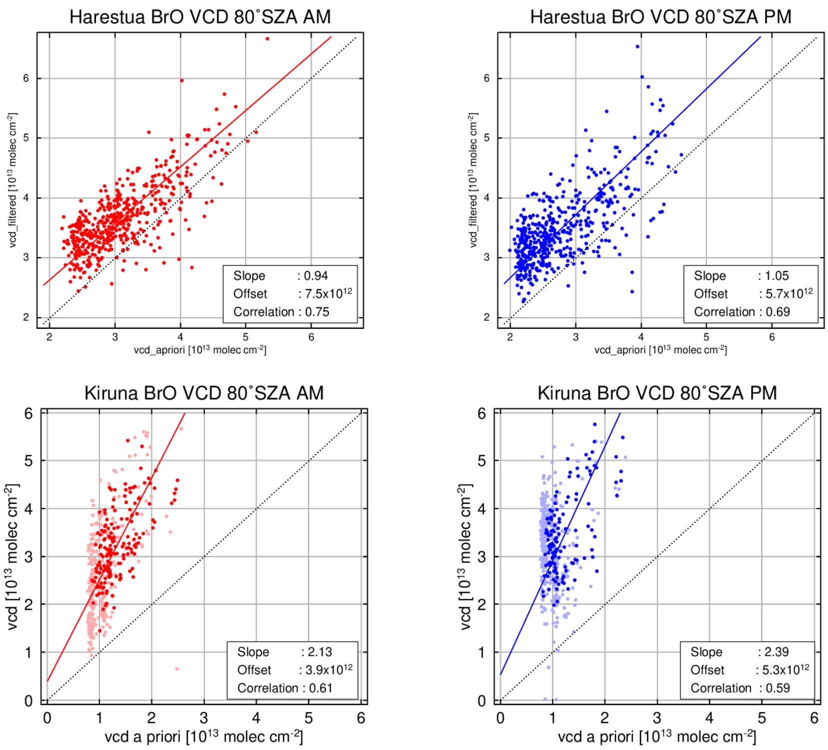

Figure 17: Correlation of BrO columns from the BASCOE a priori (x-axis) and the retrieved profiles (y-axis) for Harestua (top) and Kiruna (bottom). AM results are shown left, PM results right. The dotted line is the 1:1 line, the coloured line a linear RMA regression through all unflagged values (full colours in Kiruna plots).

Another view of the same data is shown in Figure 17, which presents scatter plots of retrieved versus a priori columns. While for Harestua the agreement looks good and the main difference is an offset of less than 1×10^{13} molec cm^{-2}, the data for Kiruna also show a large difference in slope.

In summary, modelled and retrieved BrO columns in Harestua agree remarkably well, with mainly a constant offset. For Kiruna, this is not the case, and model columns are much smaller than retrieved columns. As shown in section 7, TROPOMI satellite columns for Harestua are even larger than the ground-based retrievals, and only slightly lower for Kiruna. There is no indication in ground-based and satellite data of a large difference in BrO columns between the two stations. This suggests that the BASCOE data used as a priori underestimates BrO columns in Kiruna and, presumably, at high latitudes in general. It would be interesting to compare this with other models (CAMS, SLIMCAT) if available.

9 Evaluation of the processing performance

One day of Bascoe simulations with a 10 min time step take about 20 min on 24 processors. The dependence on the time step is approximately linear, see also Fig. 5 in the ATBD. Since the model is global, this computation has to be performed only once for all stations.

The profile retrieval algorithm utilizes Python's high-level interface ProcessPoolExecutor (part of the standard library) for running CPU-bound tasks using multiple processes. Using 16 processes, we can process 1 year of data at a single retrieval SZA in approximately 1 h.

The data volume of 1 year of Bascoe data for 1 station is about 65 MB, and the data volume of a profile file for one station covering 1 year at 3 retrieval SZAs is about 570 MB.

10 Summary and Conclusions

A first quick-look evaluation of the FRM4DOAS BrO data set was performed on data from the stations in Harestua and Kiruna. The data appear to be self-consistent, show the right magnitude and seasonality, and the flags provided work well, at least for Harestua. Data for Kiruna show much greater variability, either due to a lower signal-to-noise ratio or to the more complex photochemical regime at high latitude. There is also a less clear correlation with tropopause height than expected for Kiruna, again pointing to issues with this station. For Harestua, the consistency between retrieved and model data is remarkably good, but in Kiruna, the BASCOE model predicts very low columns, which is not in agreement with the retrievals and also not with TROPOMI satellite data.

Data from more stations and different years will be analysed in the next phase of the FRM4DOAS project, and this should provide more conclusive information on the overall quality of the BrO profile retrievals and their applicability to Altius validation.

11 References

AIRS Science Team/Joao Teixeira, AIRS/Aqua L3 Daily Standard Physical Retrieval (AIRS+AMSU) 1 degree x 1 degree V006, Greenbelt, MD, USA, Goddard Earth Sciences Data and Information Services Center (GES DISC), Accessed: [Data Access 04.07.2026], 10.5067/Aqua/AIRS/DATA301, 2013.

Aliwell, S. R., Van Roozendael, M., Johnston, P. V., Richter, A., Wagner, T., Arlander, D. W., Burrows, J. P., Fish, D. J., Jones, R. L., Tørnkvist, K. K., Lambert, J.-C., Pfeilsticker, K., and Pundt, I.: Analysis for BrO in zenith-sky spectra: An intercomparison exercise for analysis improvement, J. Geophys. Res., 107(D14), 4199, doi:10.1029/2001JD000329, 2002.

Bogumil, K., Orphal, J., Homann, T., Voigt, S., Spietz, P., Fleischmann, O., Vogel, A., Hartmann, M., Bovensmann, H., Frerik, J., and Burrows, J. P.: Measurements of molecular absorption spectra with the SCIAMACHY pre-flight model: instrument characterization and reference data for atmospheric remote sensing in the 230–2380 nm region, J. Photoch. Photobio. A, 157, 167–184, https://doi.org/10.1016/S1010-6030(03)00062-5, 2003.

Burrows, J. P., A. Richter, A. Dehn, B. Deters, S. Himmelmann, S. Voigt, and J. Orphal, Atmospheric remote-sensing reference data from GOME, 2, Temperature-dependent absorption cross-sections of O3 in the 231–794 nm range, J. Quant. Spectrosc. Radiat. Transfer, 61, 509 – 517, 1999.

GMAO (Global Modeling and Assimilation Office), MERRA-2 tavg1_2d_slv_Nx: 2d,1-Hourly,Time-Averaged,Single-Level,Assimilation,Single-Level Diagnostics V5.12.4, Greenbelt, MD, USA, Goddard Earth Sciences Data and Information Services Center (GES DISC), Accessed: [04.07.20], 10.5067/VJAFPLI1CSIV, 2015.

Greenblatt, G. D., J. J. Orlando, J. B. Burkholder, and A. R. Ravishankara, Absorption measurements of oxygen between 330 and 1140 nm, J. Geophys.Res., 95, 18,577–18,582, 1990.

Harder, J. W., J. W. Brault, P. V. Johnston, and G. H. Mount, Temperature dependent NO2 cross sections at high spectral resolution, J. Geophys. Res., 102, 3861– 3879, 1997.

Hendrick, F., P. V. Johnston, K. Kreher, C. Hermans, M. De Maziére, and M. Van Roozendael, One decade trend analysis of stratospheric BrO over Harestua (60°N) and Lauder (45°S) reveals a decline, Geophys. Res. Lett., 35, doi: 10.1029/2008GL034154, 2008.

Hendrick, F., A. Rozanov, P. V. Johnston, H. Bovensmann, M. De Maziére, C. Fayt, C. Hermans, K. Kreher, W. Lotz, B.-M. Sinnhuber, N. Theys, A. Thomas, J. P. Burrows, and M. Van Roozendael, Multi-year comparison of stratospheric BrO vertical profiles retrieved from SCIAMACHY limb and ground-based UV-visible measurements, Atmospheric Measurement Techniques, doi: 10.5194/amt-2-273-2009, 2009.

/273/2009/.Kromminga, H., Orphal, J., Spietz, P., Voigt, S., and Burrows, J.: New measurements of OClO absorption cross-sections in the 325–435 nm region and their temperature dependence between 213 and 293 K, J. Photoch. Photobio. A, 157, 149–160, https://doi.org/10.1016/S1010-6030(03)00071-6, 2003.

Puķīte, J. and Wagner, T.: Quantification and parametrization of non-linearity effects by higher-order sensitivity terms in scattered light differential optical absorption spectroscopy, Atmos. Meas. Tech., 9, 2147–2177, https://doi.org/10.5194/amt-9-2147-2016, 2016.

Puķīte, J., Kühl, S., Deutschmann, T., Platt, U., and Wagner, T.: Extending differential optical absorption spectroscopy for limb measurements in the UV, Atmos. Meas. Tech., 3, 631–653, https://doi.org/10.5194/amt-3-631-2010, 2010.

Seo, S., Richter, A., Blechschmidt, A.-M., Bougoudis, I., and Burrows, J. P.: First high-resolution BrO column retrievals from TROPOMI , Atmos. Meas. Tech. , 12 , 2913-2932, https://doi.org/10.5194/amt-12-2913-2019, 2019.

Sihler, H., Platt, U., Beirle, S., Marbach, T., Kühl, S., Dörner, S., Verschaeve, J., Frieß, U., Pöhler, D., Vogel, L., Sander, R., and Wagner, T.: Tropospheric BrO column densities in the Arctic derived from satellite: retrieval and comparison to ground-based measurements, Atmos. Meas. Tech., 5, 2779–2807, https://doi.org/10.5194/amt-5-2779-2012, 2012.

Thalman, R. and Volkamer, R.: Temperature dependent absorption cross-sections of O2–O2 collision pairs between 340 and 630 nm and at atmospherically relevant pressure, Phys. Chem. Chem. Phys., 15, 15371, https://doi.org/10.1039/c3cp50968k, 2013.

Theys, N., Van Roozendael, M., Errera, Q., Hendrick, F., Daerden, F., Chabrillat, S., Dorf, M., Pfeilsticker, K., Rozanov, A., Lotz, W., Burrows, J. P., Lambert, J.-C., Goutail, F., Roscoe, H. K., and De Mazière, M.: A global stratospheric bromine monoxide climatology based on the BASCOE chemical transport model, Atmos. Chem. Phys., 9, 831–848, https://doi.org/10.5194/acp-9-831-2009, 2009.

Vandaele, A.-C., C. Hermans, P. C. Simon, M. Carleer, R. Colin, S. Fally, M.-F. Merienne, A. Jenouvrier, and B. Coquart, Measurements of the NO2 absorption cross-section from 42,000 cm^{-1} to 10,000 cm^{-1} (238 – 1000 nm) at 220 K and 294 K, J. Quant. Spectrosc. Radiat. Transfer, 59, 171–184, 1998.

Vandaele, A. C., et al. (2005), An intercomparison campaign of ground-based UV-visible measurements of NO2, BrO, and OClO slant columns: Methods of analysis and results for NO2, J. Geophys. Res., 110, D08305, doi:10.1029/2004JD005423.

Wagner, T., Beirle, S., Donner, S., Enell, C.-F., Gu, M., Lauster, B., Platt, U., Pukite, J., Raffalski, U., and Ziegler, S.: Characterisation of spectroscopic properties of DOAS instruments using high-resolution solar spectra, Atmos. Meas. Tech., 19, 4065–4097, https://doi.org/10.5194/amt-19-4065-2026, 2026.

Wilmouth, D. M., Hanisco, T. F., Donahue, N. M., and Anderson, J. G.: Fourier transform ultraviolet spectroscopy of the $A(^2\Pi_{3/2}) \leftarrow X(^2\Pi_{3/2})$ transition of BrO, J. Phys. Chem., 103,8935–8945, 1999.